Dalton Transactions

ROYAL SOCIETY OF CHEMISTRY

PAPER

Published on 05 August 2026
Licensed under CC-BY 4.0

Check for updates

Cite this: DOI: 10.1039/d6dt01176d

Molecular multinuclear praseodymium manganese crown-ether coordination compounds

Maxime A. Bonnin, Silke Wolf and Claus Feldmann *

Received 18th May 2026,
Accepted 4th August 2026

DOI: 10.1039/d6dt01176d

rsc.li/dalton

Crown-ether-coordination compounds of praseodymium(III), manganese(II) and the crown ether 18-crown-6 ($(C_2H_4O)_6$, 18c6) are prepared in $[Bu_3MeN][NTf_2]$ ($[Bu_3MeN]^+/[(C_4H_9)_3(CH_3)N]^+$: tributylmethylammonium; $[NTf_2]^-/[(CF_3SO_2)_2N]^-$: bis(trifluoromethylsulfonyl)amide) as an ionic liquid. Specifically, the reaction of $PrCl_3$, PrI_3, $MnCl_2$ or MnI_2 with 18c6 at 80–100 °C results in the novel compounds $[PrCl_3(18c6)]$ (**1**), $[MnCl_2(18c6)]$ (**2**), $[Bu_3MeN][PrI_2(18c6)][MnI_4]$ (**3**), $[Bu_3MeN]_2[MnI_4]$ (**4**), $[Bu_3MeN]_2[(Pr(I_{0.82}Cl_{0.18})Cl(18c6))_2][MnI_4]_2$ (**5**) and $[(PrCl_2(18c6)MnI_3)_2]$ (**6**). They contain mononuclear arrangements of Pr^{3+} (**1**) and Mn^{2+} (**2**) with 18c6. **3** and **5** contain both Pr^{3+} and Mn^{2+} in a single compound but in different molecular building units ($[PrI_2(18c6)]^+$, $[(Pr(I_{0.82}Cl_{0.18})Cl(18c6))_2]^+$, and $[MnI_4]^{2-}$) with a great distance between them (Pr–Mn > 700 pm). Finally, **6** represents the first crown-ether coordination compound with Pr^{3+} and Mn^{2+} in a single tetranuclear molecule. All title compounds are characterized by X-ray diffraction (single crystals, powder diffraction with Rietveld analysis), infrared spectroscopy, thermal analysis, and photoluminescence spectroscopy. **2–5**, even when containing Pr^{3+} (**3** and **5**), show typical luminescence of Mn^{2+}, whereas **1** and **6** show Pr^{3+}-type transitions, with **6** showing particularly intense emission. $Pr^{3+} \rightarrow Mn^{2+}$ energy transfer is not observed, which can be ascribed to the specific distances between the luminescent centers (**3** and **5**) or the symmetry of the molecule (**6**).

1. Introduction

Crown-ether coordination compounds of di- and trivalent lanthanide cations have turned out to be interesting with regard to their structural, coordinative, magnetic and luminescent features, in general.[1] Magnetic properties comprise ferromagnetic coupling as well as single-molecule magnets such as $[Dy(18c6)L_2][I_3]$ (L: ligand), $[TmI_2(18c6)]$ or $[Ln(NO_3)_3(18c6)]$ (Ln: Ce, Pr, Nd) with slow spin-relaxation at low temperature.[1a,c,2] Aiming at luminescence, compounds such as $[(Yb_2L_3)Tb_2]$ (L_3: bis-pyridylphosphonated-pyclen), $[SmI_2(18c6)]$, $[EuI_2(18c6)]$, $[TmI_2(18c6)]$ and $[Eu(15c5)(terpy)]Cl_3$ (terpy = 2,2′,6′,2″-terpyridine) were reported, partly with intense emission and high quantum yields (>80%).[1b,c,2b,3] Besides the crown ether, however, the lanthanide is often also coordinated by OH, H_2O or other ligands that can quench the emission due to competitive vibrational loss processes partly or even completely.[4] Specifically for luminescence, crown-ether coordination compounds can show specific advantages related to coordination and bonding.[1b,c,2b,3] This comprises rigid bonding of the lanthanide as a luminescent center by the crown ether, the absence of ligands with high-energy vibronic transitions (*i.e.*, O–H, N–H, C=O) or the separation of single lanthanides or pairs of lanthanides by a great distance from neighbouring luminescent centers to avoid concentration quenching.[1b,c,3c,5] With regard to the crown ether, 18c6 has been applied most often, which can be attributed to its high stability and strong coordination.[1–3] Due to the ring-opening of 18c6 of about 300 pm,[6] coordination of divalent lanthanides is observed more often (*e.g.* Eu^{2+}: 125 pm, C.N. 8),[7] whereas trivalent lanthanides exhibit a non-optimal small size (*e.g.* Eu^{3+}: 107 pm, Pr^{3+}: 113 pm, C.N. 8).[7] Moreover, the higher charge of trivalent lanthanides and their high Lewis acidity are less favourable and can even lead to a splitting of the crown ether.[8]

Whereas most of the studies on luminescent crown-ether compounds are related to $Eu^{2+/3+}$, $Sm^{2+/3+}$, Tm^{3+} or Yb^{3+} as luminescent centers,[1–4] Pr^{3+} has rarely been examined until now.[2c,9] However, Pr^{3+} is interesting in many ways. Pr^{3+} usually shows green emission *via* the $^3P_0 \rightarrow {}^3H_4$ transition and can be excited *via* $5d^04f^2 \rightarrow 5d^14f^1$ as a parity-allowed process.[8] Besides green emission, Pr^{3+} is also suitable for red ($^3P_0 \rightarrow {}^3H_6$) or UV ($^1S_0 \rightarrow {}^3H_4$) emission, depending on the specific coordination and bonding scenario.[8,10] Crown-ether coordination compounds with Pr^{3+} were also reported for the removal of oxygen,[9a] slow magnetic relaxation,[2c] or as fluorescence sensors.[9c] Finally, Pr^{3+} is well-known for efficient energy transfer to Mn^{2+} as another widely applied luminescent center.[11] Even a two-photon emission – so-called quantum

Institute of Inorganic Chemistry, Karlsruhe Institute of Technology (KIT), Engesserstrasse 15, D-76131 Karlsruhe, Germany. E-mail: claus.feldmann@kit.edu

cutting – was considered for the Pr^{3+}–Mn^{2+} couple.[12] Taking the potentially interesting properties of Pr^{3+}-containing crown-ether compounds as well as the limited knowledge on such compounds into account, we here examine the options to synthesize crown-ether coordination compounds with Pr^{3+} and Mn^{2+}. Specifically, a combination of both metal cations in a single molecular compound with short Pr–Mn distance could be interesting in terms of the coordinative scenario and promising for luminescence.[8,11,12] Moreover, molecular crown-ether coordination compounds containing two different metals as luminescent centers have rarely been reported until now. In the following, we explore the reaction of $PrCl_3$/PrI_3 and $MnCl_2$/MnI_2 with 18c6 to obtain crown-ether coordination compounds with Pr^{3+} and Mn^{2+}. As a result, the novel compounds $[PrCl_3(18c6)]$ (**1**), $[MnCl_2(18c6)]$ (**2**), $[Bu_3MeN][PrI_2(18c6)][MnI_4]$ (**3**), $[Bu_3MeN]_2[MnI_4]$ (**4**), $[Bu_3MeN]_2[(Pr(I_{0.82}Cl_{0.18})Cl(18c6))_2][MnI_4]_2$ (**5**), and $[(PrCl_2(18c6)MnI_3)_2]$ (**6**) were obtained, which were characterized with regard to composition, structure, and thermal and luminescence properties.

2. Experimental section

2.1 General

The starting materials $PrCl_3$ (99.99%, Sigma-Aldrich), PrI_3 (99.9%, Fisher Scientific), $MnCl_2$ (99.99%, Fisher Scientific) and MnI_2 (99.99%, Sigma-Aldrich) were used as purchased. 18-Crown-6 (18c6, 99%, Sigma-Aldrich) was dried for several days under reduced pressure ($<10^{-3}$ mbar) at 100 °C before use. The ionic liquid $[Bu_3MeN][NTf_2]$ was prepared by reaction of $[Bu_3MeN]Cl$ with $Li[NTf_2]$.[13] The ionic liquid was extracted with CH_2Cl_2 to remove excess starting materials and thereafter washed with water three times to remove LiCl as a by-product. Finally, the ionic liquid was dried for several days under reduced pressure ($<10^{-3}$ mbar) at 100 °C before use. All reactants were used and stored in an argon glovebox (MBraun UNILab, O_2/H_2O < 1 ppm). Standard Schlenk techniques were used for all reactions. Glass ampoules were evacuated ($<10^{-3}$ mbar), heated and flushed with argon three times to remove all moisture. To remove the ionic liquid after the syntheses, the crystals of **1–6** were washed with small portions of cold CH_2Cl_2 (0 °C).

2.2 Synthesis of compounds

$[PrCl_3(18c6)]$ (1). 50.0 mg (0.20 mmol) of $PrCl_3$ and 53.4 mg (0.20 mmol) of 18c6 were reacted in 300 μL of $[Bu_3MeN][NTf_2]$ at 80 °C for 14 d. After cooling to room temperature with a rate of 1 K h^{-1}, **1** was obtained as small colourless, needle-shaped crystals with a yield of about 40%. The yield is mainly limited due to part of the crown ether remaining dissolved in the ionic liquid.

$[MnCl_2(18c6)]$ (2). 50.0 mg (0.20 mmol) of $PrCl_3$, 25.4 mg (0.20 mmol) of $MnCl_2$ and 53.4 mg (0.20 mmol) of 18c6 were reacted in 300 μL of $[Bu_3MeN][NTf_2]$ at 80 °C for 14 d. After cooling to room temperature with a rate of 1 K h^{-1}, colourless crystals were obtained with a yield of about 20%. The reaction can also be performed without the addition of $PrCl_3$. The yield is mainly limited due to part of the crown ether remaining dissolved in the ionic liquid.

$[Bu_3MeN][PrI_2(18c6)][MnI_4]$ (3) and $[Bu_3MeN]_2[MnI_4]$ (4). 50.0 mg (0.09 mmol) of PrI_3, 29.6 mg (0.09 mmol) of MnI_2 and 25.3 mg (0.09 mmol) of 18c6 were reacted in 300 μL of $[Bu_3MeN][NTf_2]$ at 80 °C for 14 d. After cooling to room temperature with a rate of 1 K h^{-1}, colorless crystals of **3** and green crystals of **4** were obtained with a yield of about 40% for each compound. Attempts to prepare **3** as a pure compound failed. **4** was always obtained a by-product and **3** and **4** can be easily differentiated based on the different colours of the compounds.

$[Bu_3MeN]_2[(Pr(I_{0.82}Cl_{0.18})Cl(18c6))_2][MnI_4]_2$ (5). 100.0 mg (0.20 mmol) of PrI_3, 24.1 mg (0.20 mmol) of $MnCl_2$ and 50.6 mg (0.20 mmol) of 18c6 were reacted in 300 μL of $[Bu_3MeN][NTf_2]$ at 100 °C for 14 d. After cooling to room temperature with a rate of 1 K h^{-1}, colourless crystals of **5** were obtained with a yield of about 40%.

$[(PrCl_2(18c6)MnI_3)_2]$ (6). 50.0 mg (0.20 mmol) of $PrCl_3$, 62.4 mg (0.20 mmol) of MnI_2 and 53.4 mg (0.20 mmol) of 18c6 were reacted in 300 μL of $[Bu_3MeN][NTf_2]$ at 100 °C for 14 d. After cooling to room temperature with a rate of 1 K h^{-1}, colorless crystals of **6** were obtained with a yield of about 50%. The yield is mainly limited due to part of the crown ether remaining dissolved in the ionic liquid.

2.3 Analytical methods

Detailed information regarding the applied analytical methods can be found in the SI.

3. Results and discussion

3.1 Synthesis and crystal structures

All title compounds were prepared by heating the respective metal halides ($PrCl_3$, PrI_3, $MnCl_2$, and MnI_2) and 18c6 at mild temperature (80–100 °C) for two weeks in $[Bu_3MeN][NTf_2]$ (Bu_3MeN: tributylmethylammonium; NTf_2: bis(trifluormethylsulfonyl)amide) as an ionic liquid (Fig. 1). The ionic liquid, on the one hand, supports the dissolution of the metal halides and, on the other hand, serves as an inert solvent.[14] Besides the thermal stability of the ionic liquid, a specific advantage is related to the weakly coordinating properties of $[Bu_3MeN][NTf_2]$, so that the metal salts show reasonable solubility for syntheses but only weak coordination of Pr^{3+} or Mn^{2+} with the $[NTf_2]^-$ anion.[14] Thus, the weakly coordinating properties of the ionic liquid promote coordination of Pr^{3+}/Mn^{2+} with 18c6 and allow the avoidance of the formation of solvato complexes as, for instance, with conventional solvents like THF or acetonitrile. However, a particular disadvantage of the ionic liquid is the difficult separation of the title compounds from the ionic liquid after synthesis as the solubilities of the title compounds and ionic liquid are often very similar. To address this concern, we used small portions of cold CH_2Cl_2 (0 °C) to wash the crystals of **1–6** and to remove most of the

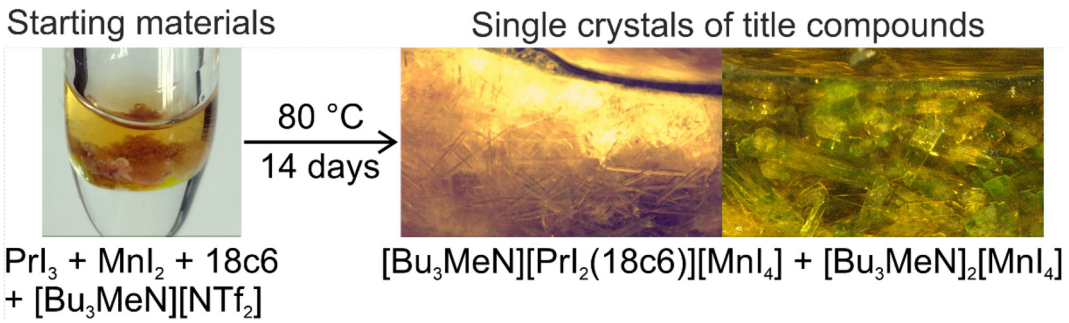

Fig. 1 Illustration of the ionic-liquid-based synthesis of **1–6** with the examples of $[Bu_3MeN][PrI_2(18c6)][MnI_4]$ (**3**) and $[Bu_3MeN]_2[MnI_4]$ (**4**): (a) photo of starting materials in $[Bu_3MeN][NTf_2]$; and (b) photos of colourless single crystals of **3** and greenish single crystals of **4** after the synthesis.

ionic liquid. However, adsorption of the remaining ionic liquid on the crystal surfaces can hardly be avoided.

With the aforementioned conditions, the novel crown-ether coordination compounds $[PrCl_3(18c6)]$ (**1**), $[MnCl_2(18c6)]$ (**2**), $[Bu_3MeN][PrI_2(18c6)][MnI_4]$ (**3**), $[Bu_3MeN]_2[MnI_4]$ (**4**), $[Bu_3MeN]_2[(Pr(I_{0.82}Cl_{0.18})Cl(18c6))_2][MnI_4]_2$ (**5**) and $[(PrCl_2(18c6)MnI_3)_2]$ (**6**) were obtained by heating the starting materials in $[Bu_3MeN][NTf_2]$ at 80–100 °C for 2 weeks (Fig. 1). While the reaction was fast as such, a duration of two weeks turned out to be optimal to promote crystal growth. Due to the moisture sensitivity of the starting materials and the title compounds, all handling and manipulation were performed under inert conditions (argon or nitrogen), using gloveboxes or Schlenk techniques.

Before jointly reacting Pr^{3+} and Mn^{2+} with 18c6, we evaluated the reactions of each single cation with the crown ether. Specifically, $PrCl_3$ and $MnCl_2$ were reacted in $[Bu_3MeN][NTf_2]$ and resulted in the mononuclear crown-ether coordination compounds $[PrCl_3(18c6)]$ (**1**) and $[MnCl_2(18c6)]$ (**2**). According to single-crystal structure analysis and PXRD with Rietveld refinement, both compounds crystallize in the monoclinic space group $P2_1/c$ (SI: Table S1 and Fig. S1, S2, and S10a and b). They consist of non-charged molecular units with Pr^{3+} (**1**) and Mn^{2+} (**2**) centrally coordinated by 18c6 (Fig. 2). In the unit cell of $[MnCl_2(18c6)]$ (**2**), two symmetry independent, very similar molecular units are found. Whereas Pr^{3+} is coordinated by one Cl^- in one hemisphere and two Cl^- in the opposite

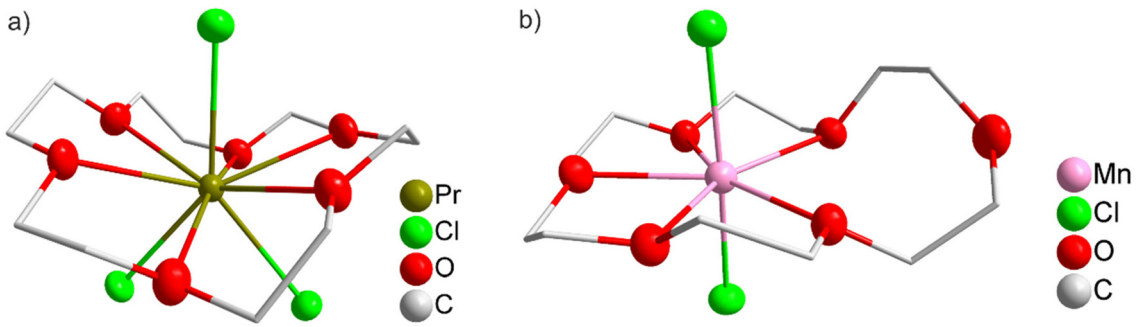

Fig. 2 Molecular structures of the mononuclear crown-ether coordination compounds: (a) $[PrCl_3(18c6)]$ (**1**) and (b) $[MnCl_2(18c6)]$ (**2**) (only one of the two molecular units is shown).

Table 1 Selected distances (in pm) in compounds **1–6**

Compound	Pr–O/Mn–O	Pr–Cl/Pr–I	Mn–Cl/Mn–I
$[PrCl_3(18c6)]$ (**1**)	258.2–266.5 (Pr)	278.2–280.0 (Cl)	—
$[MnCl_2(18c6)]$ (**2**)	231.0–239.7 (Mn) 246.0, 257.7 (Mn)	—	242.2–244.7 (Cl)
$[Bu_3MeN][PrI_2(18c6)][MnI_4]$ (**3**)	251.4–256.2 (Pr)	307.4–308.6 (I)	269.9–273.3 (I)
$[Bu_3MeN]_2[MnI_4]$ (**4**)	—	—	263.5–275.2 (I)
$[Bu_3MeN]_2[(Pr(I_{0.82}Cl_{0.18})Cl(18c6))_2][MnI_4]_2$ (**5**)	253.8–258.6 (Pr)	316.2 (I) 281.7–282.9 (Cl[a])	260.5–279.5 (I)
$[(PrCl_2(18c6)MnI_3)_2]$ (**6**)	254.5–258.3 (Pr)	288.7, 292.2 (Cl)	247.8 (Cl) 267.4–273.9 (I)

[a] Pr–Cl distances for bridging Cl with 85% occupancy.

hemisphere (Pr–Cl: 278.2(1)–280.0(1) pm; Table 1), Mn^{2+} is axially coordinated by two Cl^- (Mn–Cl: 242.2(1), 244.7(1) pm). The $PrCl_3$ unit nearly forms a trigonal-squared arrangement with larger Cl_{trans}–Pr–Cl_{trans} angles (139.8(1)–141.5(1)°) than the Cl_{cis}–Pr–Cl_{cis} angle (78.4(1)°, Fig. 2a). The $MnCl_2$ units are almost linear (Cl–Mn–Cl: 172.6(1)°, 176.4(1)°, Fig. 2b). With regard to the crown ether, the larger Pr^{3+} (*r*: 113 pm, C.N. 8) shows endocyclic coordination to all oxygen atoms of 18c6 (Pr–O: 258.2(3)–266.5(3) pm), whereas the smaller Mn^{2+} (*r*: 96 pm, C.N. 8) only coordinates to 5 oxygen atoms of 18c6 with four similar distances (Mn–O: 231.0(2)–239.7(2) pm) and one slightly elongated distance (Mn–O: 246.0(2) and 257.7(2) pm), leaving the final oxygen atom non-coordinated with a substantially longer Mn–O distance (437.3(2) and 463.6(1) pm) (Table 1 and Fig. 2). Although **1** with Pr^{3+} is a new compound, in principle, comparable compounds with other lanthanides were described before (*e.g.*, La^{3+}, $Eu^{2+,3+}$, Sm^{2+}, and Tm^{3+}).[2,3,15] Specifically using $PrCl_3$ as a starting material, only [$PrCl_3$(15c5)] and [$PrCl_2$(dibenzo-18c6)(H_2O)][$SbCl_6$]·0.5MeOH·0.5MeCN are known as examples.[16] Compounds comparable with **2** were realized with [$MnCl_2$(15c5)] containing the smaller crown ether 15c5 as well as the heavier halide iodine.[3c,17]

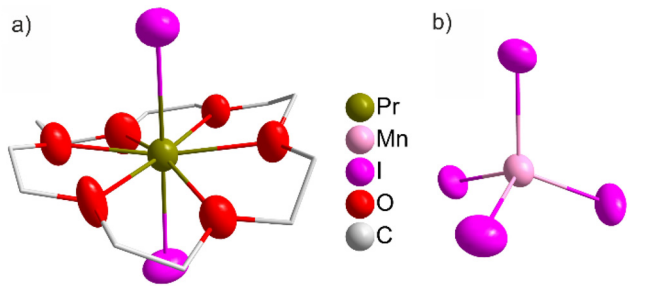

Fig. 3 Molecular structure of the crown-ether coordination compound [Bu_3MeN][PrI_2(18c6)][MnI_4] (**3**): (a) [PrI_2(18c6)]$^+$ cation and (b) [MnI_4]$^{2-}$ anion; [Bu_3MeN]$_2$[MnI_4] (**4**) is not displayed as the Mn^{2+}-containing building unit comprises [MnI_4]$^{2-}$ anions similar to **3**.

After reaction of $PrCl_3$ with 18c6 as well as that of $MnCl_2$ with 18c6, with the result that both cations Pr^{3+} and Mn^{2+} are coordinated by 18c6, we mixed equivalent amounts of $PrCl_3$ and $MnCl_2$ and reacted them together in [Bu_3MeN][NTf_2]. However, these attempts only again led to compounds **1** and **2**. As the synthesis was not successful with the more Lewis-acidic and more ionic $PrCl_3$/$MnCl_2$, we repeated the synthesis with the less Lewis-acidic and less ionic PrI_3/MnI_2, which resulted in [Bu_3MeN][PrI_2(18c6)][MnI_4] (**3**) and [Bu_3MeN]$_2$[MnI_4] (**4**). They crystallized in the space groups $P2_1/c$ (**3**) and $P2_1/n$ (**4**) (**4** with $P2_1/n$ as $P2_1/c$ would lead to a β angle > 120°; SI: Tables S1 and S2 and Fig. S3–S5). The space group and crystal structure were confirmed by X-ray powder diffraction (XRD) with Rietveld refinement (Fig. S10c and d). Despite the different temperatures and ratios of the starting materials, all attempts to prepare **3** as a pure compound failed, and **4** was always

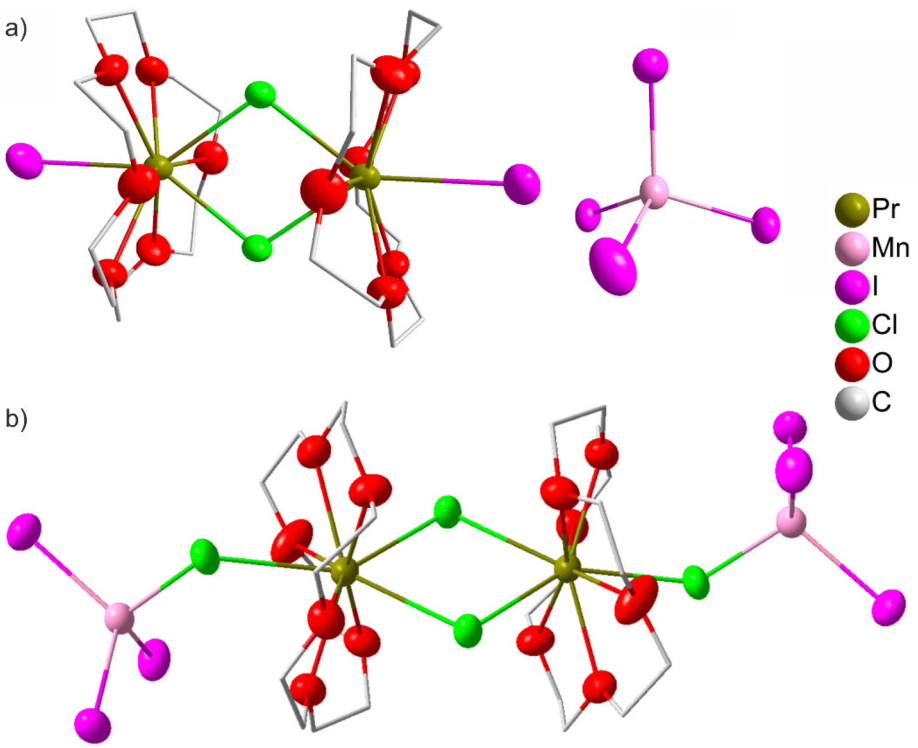

Fig. 4 Molecular structures of the multinuclear crown-ether coordination compounds: (a) [Bu_3MeN]$_2$[(Pr($I_{0.82}Cl_{0.18}$)Cl(18c6))$_2$][MnI_4]$_2$ (**5**) with the dinuclear [(Pr($I_{0.82}Cl_{0.18}$)Cl(18c6))$_2$]$^+$ cation (disorder and split occupancies shown in the SI: Fig. S7) and (b) tetranuclear molecule [($PrCl_2$(18c6)MnI_3)$_2$] (**6**) (disorder shown in the SI: Fig. S9).

obtained as a side-phase. Due to the colourless crystals of **3** and the greenish colour of **4**, crystals of both compounds can be easily differentiated (Fig. 1).

As intended, **3** contains both luminescent centers with Pr^{3+} in a $[PrI_2(18c6)]^+$ cation, Mn^{2+} in a $[MnI_4]^{2-}$ anion and a $[Bu_3MeN]^+$ cation (Fig. 3). Comparable to **1**, the $[PrI_2(18c6)]^+$ cation shows Pr^{3+} centrally coordinated by 18c6 (Pr–O: 251.4(10)–256.2(12) pm; Table 1). Moreover, Pr^{3+} is coordinated by two iodine atoms (Pr–I: 307.4(2), 308.6(2) pm) with an almost linear arrangement (I–Pr–I: 173.8(1)°). The isolated $[MnI_4]^{2-}$ anion (Mn–I: 269.9(2)–273.3(2) pm) shows a distorted tetrahedral arrangement (I–Mn–I: 104.8(1)–114.1(1)°) (Fig. 3). The Mn–I distance is in good agreement with isolated $[MnI_4]^{2-}$ reported in the literature (268.3–274.3 pm).[18] Despite the fact

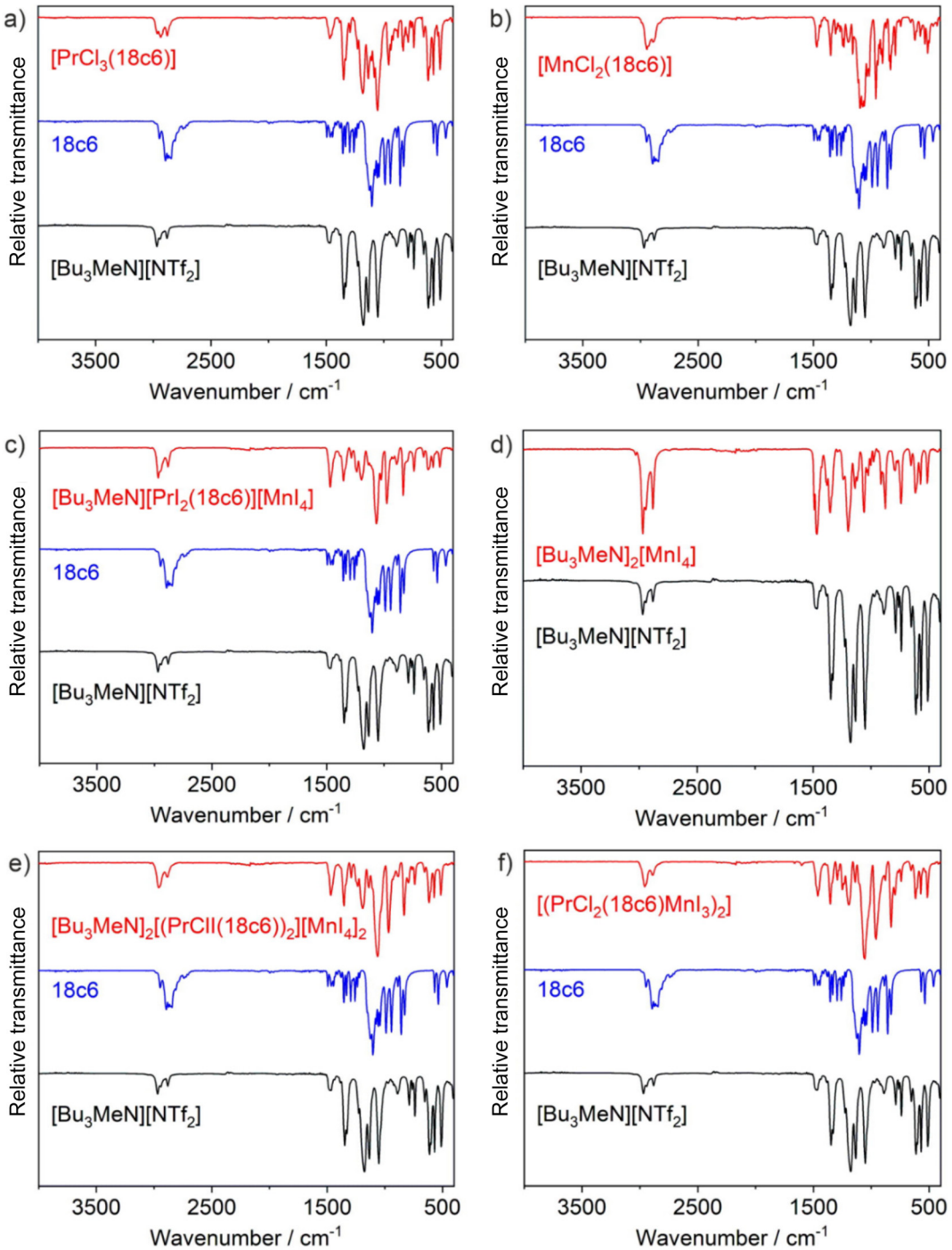

Fig. 5 Fourier-transform infrared (FT-IR) spectra of: (a) $[PrCl_3(18c6)]$ (**1**); (b) $[MnCl_2(18c6)]$ (**2**); (c) $[Bu_3MeN][PrI_2(18c6)][MnI_4]$ (**3**); (d) $[Bu_3MeN]_2[MnI_4]$ (**4**); (e) $[Bu_3MeN]_2[(Pr(I_{0.82}Cl_{0.18})Cl(18c6))_2][MnI_4]_2$ (**5**); and (f) $[(PrCl_2(18c6)MnI_3)_2]$ (**6**).

that **3** is a new compound and that it – as intended – contains Pr^{3+} and Mn^{2+} as two different luminescent centers, the relevance for luminescence is nevertheless limited as the distance between the metal cations is too large for efficient energy transfer (*e.g.*, *via* superexchange or dipole–dipole interaction) with Pr–Mn: 736.6(2) pm and Pr–Pr: 777.3(2) pm.[8,11,12] As a result, only conventional luminescence of Pr^{3+} and/or Mn^{2+} is to be expected (see section 3.2).

Besides **3**, $[Bu_3MeN]_2[MnI_4]$ (**4**) also represents a new compound (SI: Table S1 and Fig. S4, S5, and S10d). As **4** contains only Mn^{2+} as the sole luminescent center, $[Bu_3MeN]^+$ cations and distorted tetrahedral $[MnI_4]^{2-}$ anions (Mn–I: 263.5(10)–275.2(13) pm; I–Mn–I: 108.8(1)–110.8(1)°; Table 1, I with ≥80% occupancy),[18] which are similarly observed in **3** and **5**, they are not discussed in more detail.

Based on the syntheses and structures of **1–4**, Pr^{3+} obviously favours coordination with Cl^-, whereas Mn^{2+} prefers coordination with I^-. This trend follows the concept of hard acids and hard bases (HSAB concept)[19] and reflects the charges of the cations with the higher charged Pr^{3+} coordinated by the more ionic Cl^- and the lower charged Mn^{2+} coordinated by the less ionic I^-. To disrupt these preferences, we mixed chloride and iodide and reacted PrI_3 with $MnCl_2$ as well as $PrCl_3$ with MnI_2. This attempt resulted in the compounds $[Bu_3MeN]_2[(Pr(I_{0.82}Cl_{0.18})Cl(18c6))_2][MnI_4]_2$ (**5**) and $[(PrCl_2(18c6)MnI_3)_2]$ (**6**), which crystallize in the space groups $P\bar{1}$ (**5**) and $P2_1/n$ (**6**) (SI: Table S2 and Fig. S6–S9). The space group and purity were confirmed by X-ray powder diffraction (XRD) with Rietveld refinement (SI: Fig. S10e and f). Here, it must be noted that **5** shows occupancy disorder for the terminal halide with split positions of 82% I and 18% Cl. In addition, **5** shows positional disorder of 18c6 as well as of the $[Bu_3MeN]^+$ cation, which was addressed by split-atom positions with an occupancy of 50% for both positions (SI: Fig. S7).

Similar to **3**, **5** contains Pr^{3+} and Mn^{2+} as luminescent centers but again separated into two different building units with a dinuclear $[(Pr(I_{0.82}Cl_{0.18})Cl(18c6))_2]^+$ cation, the already observed $[MnI_4]^{2-}$ anion and $[Bu_3MeN]^+$ cations (Fig. 4a). The $[(Pr(I_{0.82}Cl_{0.18})Cl(18c6))_2]^+$ cation exhibits a centrally coordinated Pr^{3+} with 18c6 (Pr–O: 253.8(4)–258.6(4) pm). Furthermore, Pr^{3+} is coordinated by two chlorine atoms (Pr–Cl: 281.7(1)–282.9(1) pm), which bridge to a second Pr^{3+}. Finally, each Pr^{3+} is coordinated by a terminal halide. This site is partially occupied by iodine (82%) and chlorine (18%) (Pr–I: 316.2(2), Pr–Cl: 287.7(3) pm). The $I_{0.82}Cl_{0.18}$–Pr–(μ^2-$Cl_{2/2}$)–Pr–$I_{0.82}Cl_{0.18}$ unit is almost planar with vertical positioning of 18c6 and shows $I_{0.82}$–Pr–Cl and Cl–Pr–Cl angles of 143.4(4)–144.2(4)° and 72.2(1)°, respectively. The distorted, isolated $[MnI_4]^{2-}$ tetrahedron is similar to **3** and **4** (Mn–I: 260.5(3)–279.5(2) pm; I–Mn–I: 105.3(4)–113.7(1)°; Table 1 and Fig. 4a). The distances (specifically Pr–Mn) between the luminescent centers are again probably too long for an efficient energy transfer (Pr–Mn: 736.3(2) pm; Pr–Pr: 456.2(1) pm).

Aiming at two different luminescent centers in a molecular compound, we were finally successful with the tetranuclear $[(PrCl_2(18c6)MnI_3)_2]$ (**6**) (Fig. 4b), which represents a non-charged dimeric molecule with two Pr(18c6) units (Pr–O: 254.5(5)–258.3(5) pm), bridged *via* two chlorine atoms (Pr–Cl: 288.7(2), 292.2(2) pm; Cl–Pr–Cl_{trans}: 142.4(1)° and 145.5(1)°; Cl–Pr–Cl_{cis}: 70.8(1)°; Table 1) as well as two tetrahedral-like $MnClI_3$ units (Mn–Cl: 247.8(4) pm; Mn–I: 267.4(7)–273.9(15) pm; I–Mn–I: 104.2(2)–119.8(4)°; I–Mn–Cl: 102.2(2)–115.3(2)°; Table 1), which are bridged *via* chlorine to the Pr(18c6) units (Pr–Cl: 290.1(2) pm). With **6**, indeed the first example of a tetranuclear crown-ether coordination compound with both Pr^{3+} and Mn^{2+} in a single molecule is realized. Moreover, the distances between the luminescent centers are, in principle, short enough to allow sufficient energy transfer (Pr–Mn: 478.1(2) pm and Pr–Pr: 473.5(2) pm) most probably *via* dipole–dipole interaction.[8] Besides Pr^{3+} and Mn^{2+} with sufficient distance in a molecular compound, the rigid coordination of Pr^{3+} by the crown ether, the presence of non-inversion symmetric $MnClI_3$ units, and the presence of heavy iodine ligands can be advantageous for luminescence (Fig. 4b).

Table 2 Thermal analysis of the title compounds **1–6** (see the SI: Fig. S11–S16 for TG analyses and XRD of thermal remnants)

	TG mass loss/%		
Compound	Experimental	Calculated	Thermal remnants
$[PrCl_3(18c6)]$ (**1**)	81 (100–400)	73 (18c6, 3 HCl)	PrF_3, PrOF (MnF_2)
$[MnCl_2(18c6)]$ (**2**)	74 (100–400)	68 (18c6)	
	21 (700–1000)	19 (2 HCl)	
$[Bu_3MeN][PrI_2(18c6)][MnI_4]$ (**3**)	82 (100–400)	78 (18c6, Bu_3MeN, 5 HI)	PrOF, (MnF_2)
	8 (500–900)	9 (HI)	
$[Bu_3MeN]_2[MnI_4]$ (**4**)	84 (200–450)	81 (2 Bu_3MeN, 3 HI)	PrF_3 [a], PrOF [a] (MnF_2)
	4 (700–1000)	13 (HI)	
$[Bu_3MeN]_2[PrICl(18c6)_2][MnI_4]_2$ (**5**)[b]	70 (200–450)	74 (2 18c6, 2Bu_3MeN, 8 HI)	PrF_3, PrOF (MnF_2)
	11 (500–900)	13 (2 HI, 2 HCl)	
$[(PrCl_2(18c6)MnI_3)_2]$ (**6**)	50 (250–350)	50 (2 18c6, 3 HI)	PrF_3, PrOCl, (MnF_2)
	25 (500–900)	25 (3 HI, 2 HCl)	

The formation of fluorides and oxide fluorides can be ascribed to the remains of the ionic liquid $[Bu_3MeN][(CF_3SO_2)_2N]$ adsorbed on the crystal surfaces. MnF_2 could not be detected, most probably due to diffusion into the alumina crucible at high temperature. [a] **4** is a side phase of **3** (see section 3.1). [b] Decomposition calculated for full occupation of **5** with iodine.

3.2 Material properties

Besides X-ray diffraction based on single crystals, compounds **1–6** were additionally characterized by X-ray powder diffraction (XRD) with Rietveld refinement (SI: Fig. S10), Fourier-transform infrared (FT-IR) spectroscopy (Fig. 5), and thermogravimetry (TG) (SI: Fig. S11–S16). FT-IR spectra of **1–6** are dominated by the respective organic constituents $[Bu_3MeN]^+$ and

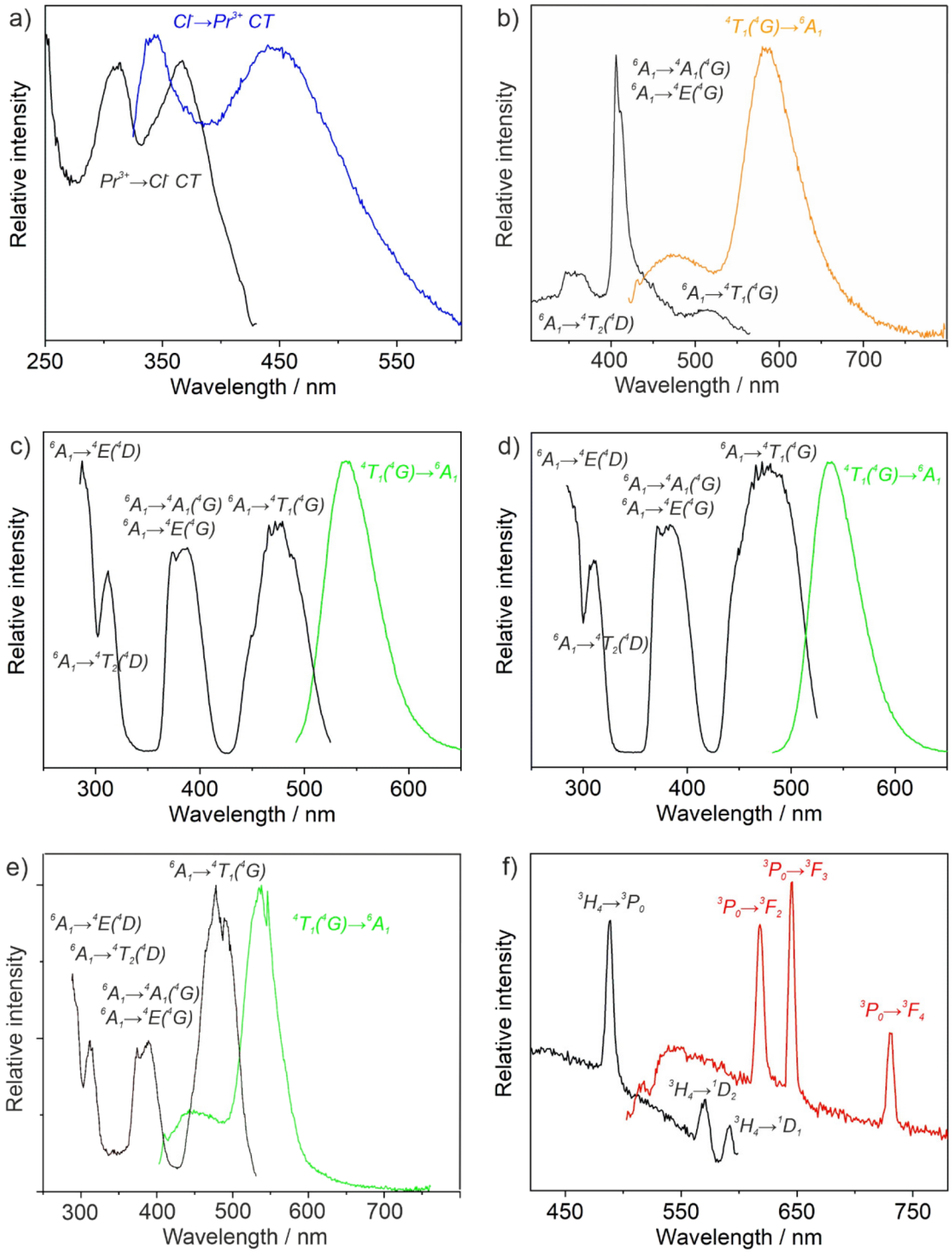

Fig. 6 Photoluminescence (PL) spectra of: (a) $[PrCl_3(18c6)]$ (**1**) with λ_{exc} = 310 nm and λ_{em} = 343 nm; (b) $[MnCl_2(18c6)]$ (**2**) with λ_{exc} = 406 nm and λ_{em} = 580 nm; (c) $[Bu_3MeN][PrI_2(18c6)][MnI_4]$ (**3**) with λ_{exc} = 467 nm and λ_{em} = 540 nm; (d) $[Bu_3MeN]_2[MnI_4]$ (**4**) with λ_{exc} = 467 nm and λ_{em} = 540 nm; (e) $[Bu_3MeN]_2[(Pr(I_{0.82}Cl_{0.18})Cl(18c6))_2][MnI_4]_2$ (**5**) with λ_{exc} = 388 nm and λ_{em} = 538 nm; and (f) $[(PrCl_2(18c6)MnI_3)_2]$ (**6**) with λ_{exc} = 488 nm and λ_{em} = 618 nm.

18c6, which were added as references (Fig. 5). Moreover, weak vibrations of $[NTf_2]^-$ are visible (ν(S=O): 1400–1200 cm^{-1}; ν(C–F): 750–500 cm^{-1}) and point to the ionic liquid used for synthesis that remains adsorbed on the crystal surfaces of the title compounds.

Thermogravimetric (TG) analysis shows one-step decomposition (**1** and **4**) or two-step decomposition (**2**, **3**, **5** and **6**) with the first step usually up to 450 °C and the second step up to 1000 °C (SI: Fig. S11–S16). The thermal decomposition can be rationalized based on the decomposition of the organic constituents ($[Bu_3MeN]^+$, 18c6). Moreover, the halides are released as HCl and HI (Table 2). Subsequent to heating, interestingly, fluorides such as PrF_3 and PrOF were identified as thermal remnants *via* XRD (Table 2; SI: Fig. S11–S16). The presence of fluoride again points to the remains of the ionic liquid $[Bu_3MeN][NTf_2]$ adsorbed on the crystal surfaces. In the presence of fluoride (due to decomposition of $[NTf_2]^-$), the formation of PrF_3 and PrOF is expected for Pr^{3+} as they represent the thermodynamically most stable phases. Finally, it must be noted that MnF_2 could not be detected – most probably due to diffusion into the alumina crucible at the high temperature of the TG analysis. In sum, the results of the TG analysis are in agreement with the chemical composition of the title compounds.

Finally, the luminescence properties of **1–6** were examined (Fig. 6). As both Pr^{3+} and Mn^{2+} are well-known luminescent centers,[8,11] in principle, visible emission can be expected for all title compounds. Specifically, d → f and f → f transitions may occur on Pr^{3+} as well as d → d transitions on Mn^{2+}.[8,11] However, the d → f transition on Pr^{3+} is typically observed only at high energy (*i.e.* <300 nm).[8,11,12]

Compounds **2–5** show characteristic Mn^{2+}-related excitation and emission with comparably broad d → d transitions (Fig. 6b–e). The emission ranges from the orange (**2**) to the green (**3–5**) spectral regime. The spectral features of **2** are different from those of **3–5** as the $^6A_1 \rightarrow {}^4E$ and $^6A_1 \rightarrow {}^4T_1$ absorptions only show low intensity, whereas the intensity of the $^6A_1 \rightarrow {}^4A_1$ absorption is high and its line-width is surprisingly narrow (Fig. 6b), which corresponds to the specific Mn^{2+} coordination with 18c6 and linearly arranged chlorine atoms like in $[MnCl_2(15c\text{-}5)]$.[16] **3–5** show luminescence originating from the MnI_4 tetrahedron like in $[(C_7H_{20}N_2)MnI_4]$.[20] A contribution of Pr^{3+} is not visible for **3** and **5** (Fig. 6c and e), which can be ascribed to the higher absorption strength of the Mn^{2+} transitions in comparison with Pr^{3+}.[8] Moreover, $Mn^{2+} \rightarrow Pr^{3+}$ energy transfer (*e.g.*, *via* superexchange or dipole–dipole interaction)[8] is not to be expected due to the distance between both luminescent centers (>700 pm). In sum, **3–5** show intense emission at room temperature; their emission intensity is nevertheless not on the level of comparable compounds such as Mn_3I_6(18-crown-6)$_2$ or Mn_2I_4(18-crown-6) with quantum yields near unity.[3c]

Pr^{3+}-related transitions are observed for compounds **1** and **6** (Fig. 6a and f). In the case of **1**, the absorption and emission are weak (Fig. 6a). Based on the energy position and bandwidth, they can be related to Pr^{3+}–Cl^- charge-transfer transitions.[21] However, **6** shows intense Pr^{3+}-based excitation and emission with narrow line width and transitions as assigned in Fig. 6f.[22] Surprisingly, neither an energy transfer $Pr^{3+} \rightarrow Mn^{2+}$ nor any Mn^{2+}-based emission was observed. In principle, the Pr^{3+}–Cl^-–Mn^{2+} bridge with a Pr–Mn distance of 478.1 pm is suitable for energy transfer (most probably dipole–dipole interaction).[8] Although the underlying mechanism cannot be clearly elucidated, the inversion symmetry of the dimeric $[(PrCl_2(18c6)MnI_3)_2]$ molecule with a center of inversion in the central Pr_2Cl_2 ring may prevent energy transfer due to the *J–J* selection rule.[8,12] To verify this hypothesis and, if possible, to establish efficient $Pr^{3+} \rightarrow Mn^{2+}$ energy transfer, a monomeric compound $[PrCl_2(18c6)MnI_3]$ would be of great interest, but is not yet experimentally available.

4. Conclusions

Aiming at crown-ether coordination compounds that contain Pr^{3+} and Mn^{2+} as luminescent centers, preferably in a single molecule, the compounds $[PrCl_3(18c6)]$ (**1**), $[MnCl_2(18c6)]$ (**2**), $[Bu_3MeN][PrI_2(18c6)][MnI_4]$ (**3**), $[Bu_3MeN]_2[MnI_4]$ (**4**), $[Bu_3MeN]_2[(Pr(I_{0.82}Cl_{0.18})Cl(18c6))_2][MnI_4]_2$ (**5**) and $[(PrCl_2(18c6)MnI_3)_2]$ (**6**) were obtained by reaction of $PrCl_3$, PrI_3, $MnCl_2$ or MnI_2 with 18c6 at 80–100 °C in the ionic liquid $[Bu_3MeN][NTf_2]$. Whereas **1** and **2** represent mononuclear compounds with Pr^{3+} or Mn^{2+} only, **3**, **5** and **6** contain both Pr^{3+} and Mn^{2+}. Structurally, coordination of Pr^{3+} with 18c6 as well as with Cl^- and coordination of Mn^{2+} with I^- are preferred. This results in $[PrI_2(18c6)]^+$, $[(Pr(I_{0.82}Cl_{0.18})Cl(18c6))_2]^+$, $[MnI_4]^{2-}$, and $[Bu_3MeN]^+$ as building units. **4** is only a side product in the synthesis of **3**. Besides the dinuclear $[(Pr(I_{0.82}Cl_{0.18})Cl(18c6))_2]^+$ cation in **5**, a tetranuclear molecule with two Pr^{3+} and two Mn^{2+} units is observed in **6** for the first time. The compounds were prepared with high purity, indicated by X-ray powder diffraction with Rietveld refinement, infrared spectroscopy and thermal analysis.

All title compounds show luminescence at room temperature. Despite the presence of Pr^{3+}, **3** and **5** only show the typical luminescence of Mn^{2+}, which can be ascribed to the higher transition strength of d → d transitions on Mn^{2+} compared to f → f transitions on Pr^{3+}. An energy transfer between Pr^{3+} and Mn^{2+} does not occur and can be related to the long distance between $[PrI_2(18c6)]^+$/$[(Pr(I_{0.82}Cl_{0.18})Cl(18c6))_2]^+$ and $[MnI_4]^{2-}$ building units with Pr–Mn > 700 pm. Surprisingly, intense Pr^{3+}-based luminescence is observed for **6**. Here, no Mn^{2+}-based emission or energy transfer $Pr^{3+} \rightarrow Mn^{2+}$ occurs although the Pr–Mn distance (478.1 pm) would be sufficient to allow energy transfer. Here, the *J–J* selection rule might lead to a forbidden energy transfer due to the inversion symmetry of the dimeric $[(PrCl_2(18c6)MnI_3)_2]$ molecule. Besides their syntheses, structure and novel composition, molecular crown-ether coordination compounds containing different luminescent metal centers can become highly interesting for luminescence applications.

Conflicts of interest

The authors declare no competing financial interest.

Data availability

Additional data regarding experiments and methods can be obtained from the supplementary information (SI) and on request from the authors.

Supplementary information: the analytical techniques, details of the single-crystal structure analysis, and further characterization of the title compounds. See DOI: https://doi.org/10.1039/d6dt01176d.

CCDC 2553955–2553960 contain the supplementary crystallographic data for this paper.[23a–f]

Acknowledgements

M. A. B. and C. F. acknowledge the Deutsche Forschungsgemeinschaft (DFG) for funding within the project "Crown-Ether-Coordination-Compounds with Unusual Structural and Optical Properties/Crown I (FE 911/14-1)". C. F. also acknowledges the Deutsche Forschungsgemeinschaft (DFG) for funding within the Collaborative Research Center 1573 "4f for Future" (project A04). Moreover, we acknowledge the Karlsruhe Nano Micro Facility (KNMF) and Prof. Dr D. Fenske and Dr A. Eichhöfer for data collection on a Stoe StadiVari diffractometer with the Ga-metal-jet source. Finally, we acknowledge A. Weis for experimental support as well as Dr C. Donsbach for supporting the crystal structure analysis of compound **5**.

References

1 (*a*) Y. Gil, A. Castro-Alvarez, P. Fuentealba, E. Spodine and D. Aravena, *Chem. – Eur. J.*, 2022, **28**, e202200336; (*b*) J. M. Zwier, H. Bazin, L. Lamarque and G. Mathis, *Inorg. Chem.*, 2014, **53**, 1854–1866; (*c*) A. P. de Silva, D. B. Fox, A. J. M. Huxley and T. S. Moody, *Coord. Chem. Rev.*, 2000, **205**, 41–57.

2 (*a*) W.-J. Xu, Q.-C. Luo, Z.-H. Li, Y.-Q. Zhai and Y.-Z. Zheng, *Adv. Sci.*, 2024, **11**, 2308548; (*b*) M. Xemard, M. Cordier, F. Molton, C. Duboc, B. Le Guennic, O. Maury, O. Cador and G. Nocton, *Inorg. Chem.*, 2019, **58**, 2872–2880; (*c*) H. Wada, S. Ooka, T. Yamamura and T. Kajiwara, *Inorg. Chem.*, 2017, **56**, 147–155.

3 (*a*) N. Hamon, L. Godec, S. Sanchez, M. Beyler, L. J. Charbonniere and R. Tripier, *Angew. Chem., Int. Ed.*, 2025, **64**, e20241460; (*b*) R. Guo, H. Liu, P. Fang, W. Yan, J. Zheng, Z. Bian and Z. Liu, *ACS Appl. Mater. Interfaces*, 2025, **17**, 42128–42138; (*c*) E. Merzlyakova, S. Wolf, S. Lebedkin, L. Bayarjargal, B. L. Neumeier, D. Bartenbach, C. Holzer, W. Klopper, B. Winkler, M. Kappes and C. Feldmann, *J. Am. Chem. Soc.*, 2021, **143**, 798–804; (*d*) M. F. Belian, G. F. De Sa, S. Alves and R. F. De Farias, *J. Coord. Chem.*, 2007, **60**, 173–183.

4 (*a*) A. Borah, S. Dey, S. K. Gupta, G. Rajaraman and R. Murugavel, *Dalton Trans.*, 2023, **52**, 8943–8955; (*b*) Y. Fan, Y. Li, X. Shu, R. Wu, S. Chen, Y. Jin, C. Xu, J. Chen, C. Huang and C. Xia, *ACS Omega*, 2021, **6**, 2156–2166; (*c*) L. Maxwell, M. Amoza and E. Ruiz, *Inorg. Chem.*, 2018, **57**, 13225–13234; (*d*) Y.-S. Ding, T. Han, Y.-Q. Hu, M. Xu, S. Yang and Y.-Z. Zheng, *Inorg. Chem. Front.*, 2016, **3**, 798–807.

5 G. Blasse and B. C. Grabmeier, *Luminescent Materials*, Springer, Berlin, 1994.

6 Z. Liu, S. K. M. Nalluri and J. F. Stoddart, *Chem. Soc. Rev.*, 2017, **46**, 2459–2478.

7 R. D. Shannon, *Acta Crystallogr., Sect. A:Found. Crystallogr.*, 1976, **32**, 751–767.

8 M. A. Bonnin, S. Leicht and C. Feldmann, *Inorg. Chem.*, 2025, **64**, 723–730.

9 (*a*) M. J. Lueckheide, M. Z. Ertem, M. A. Michon, P. Chmielniak and J. R. Robinson, *J. Am. Chem. Soc.*, 2022, **144**, 17295–17306; (*b*) W.-S. Xia, R. H. Schmehl and C.-J. Li, *Tetrahedron*, 2000, **56**, 7045–7049; (*c*) G. R. Willey, P. R. Meehan, P. A. Salter and M. G. B. Drew, *Polyhedron*, 1996, **15**, 4227–4232.

10 (*a*) B. Lin, R. Lv, Z. Ju and A. A. Ansari, *Coord. Chem. Rev.*, 2026, **549**, 217251; (*b*) J. J. van Blaaderen, C. van Aarle, D. Leibold, P. Dorenbos and D. R. Schaart, *Chem. Mater.*, 2025, **37**, 1716–1740; (*c*) X. Wang and Y. Mao, *J. Mater. Chem. C*, 2022, **10**, 3626–3646.

11 (*a*) L. Guo, T. Li, C. Zhu, H. Cheng and K. Zhang, *J. Solid State Chem.*, 2023, **317**, 123697; (*b*) X.-Y. Sun, Z. He and X. Gu, *J. Mater. Sci.*, 2018, **29**, 17217–17221; (*c*) A. Kuzmanoski, V. Pankratov and C. Feldmann, *J. Lumin.*, 2016, **179**, 555–561; (*d*) Y. Fu, G. Zhang, Z. Qi, W. Wu and C. Shi, *J. Lumin.*, 2007, **124**, 370–374; (*e*) Y. Chen, C. Shi, W. Yan, Z. Qi and Y. Fu, *Appl. Phys. Lett.*, 2006, **88**, 061906/1–061906/3.

12 A. Meijerink, R. Wegh, P. Vergeer and T. Vlugt, *Opt. Mater.*, 2006, **28**, 575–581.

13 D. R. MacFarlane, P. Meakin, J. Sun, N. Amini and M. Forsyth, *J. Phys. Chem. B*, 1999, **103**, 4164–4170.

14 (*a*) P. Wasserscheid and T. Welton, *Ionic Liquids in Synthesis*, Wiley-VCH, Weinheim, 2008; (*b*) D. Freudenmann, S. Wolf, M. Wolff and C. Feldmann, *Angew. Chem., Int. Ed.*, 2011, **50**, 11050–11060.

15 R. D. Rogers, A. N. Rollins, R. D. Etzenhouser, E. J. Voss and C. B. Bauer, *Inorg. Chem.*, 1993, **32**, 3451–3462.

16 (*a*) G. R. Willey, P. R. Meehan, P. A. Salter and M. G. B. Drew, *Polyhedron*, 1996, **15**, 4227–4232; (*b*) L. Nunez and R. D. Rogers, *J. Crystallogr. Spectrosc. Res.*, 1992, **22**, 265–269.

17 M. A. Bonnin and C. Feldmann, *Inorg. Chem.*, 2021, **60**, 14645–14654.

18 O. Schneider, E. Gerstner, F. Weller and K. Dehnicke, *Z. Anorg. Allg. Chem.*, 2000, **626**, 827–829.

19 R. G. Pearson, *Coord. Chem. Rev.*, 1990, **100**, 403–425.

20 T. Chang, T. Kou, Q. Wei, L. Wang, X. Cai, H. Su, Y. You, X. Li, X. Han, S. Han and W. W. Yu, *Chem. Eng. J.*, 2025, **521**, 166792.

21 (*a*) E. A. Mikhalyova, O. V. Khomenko, K. S. Gavrilenko and V. P. Dotsenko, *ACS Omega*, 2019, **4**, 2669–2675; (*b*) T. Q. H. Tran, M. H. Hoang, T. A. T. Doc, A. T. Le, T. H. Nguyen, T. D. Nguyen, M. T. M. A. W. Addison and V. V. Pavlishchuk, *J. Lumin.*, 2021, **237**, 118162.
22 S. Kück, *Appl. Phys. B*, 2001, **72**, 515–562.
23 (*a*) CCDC 2553955: Experimental Crystal Structure Determination, 2026, DOI: 10.5517/ccdc.csd.cc2rqlnr; (*b*) CCDC 2553956: Experimental Crystal Structure Determination, 2026, DOI: 10.5517/ccdc.csd.cc2rqlps; (*c*) CCDC 2553957: Experimental Crystal Structure Determination, 2026, DOI: 10.5517/ccdc.csd.cc2rqlqt; (*d*) CCDC 2553958: Experimental Crystal Structure Determination, 2026, DOI: 10.5517/ccdc.csd.cc2rqlrv; (*e*) CCDC 2553959: Experimental Crystal Structure Determination, 2026, DOI: 10.5517/ccdc.csd.cc2rqlsw; (*f*) CCDC 2553960: Experimental Crystal Structure Determination, 2026, DOI: 10.5517/ccdc.csd.cc2rqltx.